TRANSPARENT BOUNDARY CONDITIONS FOR THE WAVE EQUATION IN ONE DIMENSION AND FOR A DIRAC-LIKE EQUATION

M. PILAR VELASCO, DAVID USERO, SALVADOR JIMÉNEZ, LUIS VÁZQUEZ

ABSTRACT. We present a method to achieve transparent boundary conditions for the one-dimensional wave equation, and show its numerical implementation using a finite-difference method. We also present an alternative method for building the same transparent boundary conditions using a Dirac-like equation and a Spinor-like formalism. Finally, we extend our method to the three-dimensional wave equation with radial symmetry.

1. INTRODUCTION

Frequently in the study of the partial differential equations that model real phenomena it is necessary to fix artificial boundary conditions for limiting the area of study and obtaining unique and well-posed solutions. However these artificial conditions can affect to the solutions of the equations and cause non-desired effects. For example, in the particular case of the study of traveling waves by the wave equation the presence of artificial boundary conditions produces the appearance of reflected waves related to the transmitted wave and these reflected waves can spoil the perception of the phenomenon.

For solving this problem and avoiding the reflection effect caused by the artificial boundary conditions, in this work we propose transparent boundary conditions for the wave equation in one dimension. The purpose of these transparent boundary conditions is the disappearance of the reflected wave and to achieve that the whole traveling wave is transmitted.

In Section 2 we analyze the wave equation and describe the movement of the traveling wave by supposing that the whole traveling wave is transmitted without reflection, at continuous and discrete level. Considering the data of the previous section, in Section 3, we look for what conditions should verify the traveling wave in the limit of the boundary conditions for a complete transmission, at continuous and discrete level again, and we obtain numerical simulations that check the efficiency of our study. An alternative theoretical support for the construction of transparent boundary conditions by using Dirac-type equations and a spinor-like formalism is

shown in Section 4. Finally, in Section 5, we extend the problem to a particular case in three dimensions and we use the obtained results for achieving transparent boundary conditions in the case of the three-dimensional wave equation with radial symmetry.

Note that we use explicit schemes for the numerical implementations since they are quite simple and it is possible with them to preserve at local level the dispersion relations. Implicit schemes could be used as long as they also preserve this and all the necessary values lay inside the appropriate region.

The following step in this area that will be analyzed in future works is to extend these results for the cases of the wave equation in two and three dimensions.

2. Transparent boundary conditions for the wave equation in one-dimension

The solutions to the wave equation possess the property of superposition of traveling waves. We shall use this to build transparent boundary conditions.

Continuous level. We consider the classical initial value problem for the wave equation in the whole (one-dimensional) space

$$
\begin{aligned}
u_{tt} - c^2 u_{xx} = 0, \quad t \geq 0, \ x \in (-\infty, +\infty), \\
u(0, x) = f(x), \\
u_t(0, x) = g(x),
\end{aligned}
\tag{2.1}
$$

where f and g are suitable functions.

According to the D'Alembert formula, the solution to (2.1) is

$$
u(t, x) = \frac{1}{2}\left[f(x - ct) + f(x + ct)\right] + \frac{1}{2c} \int_{x-ct}^{x+ct} g(s)\, ds.
\tag{2.2}
$$

Let us suppose that G exists, a primitive function for g, and we have:

$$
\begin{aligned}
u(t, x) &= \frac{1}{2}\left[f(x + ct) + f(x - ct)\right] + \frac{1}{2c}\left[G(x + ct) - G(x - ct)\right] \\
&= \frac{1}{2}f(x + ct) + \frac{1}{2c}G(x + ct) + \frac{1}{2}f(x - ct) - \frac{1}{2c}G(x - ct).
\end{aligned}
\tag{2.3}
$$

This corresponds to the superposition of two traveling waves $v(t, x)$ and $w(t, x)$ given by:

$$
v(t, x) = \frac{1}{2}f(x + ct) + \frac{1}{2c}G(x + ct),
\tag{2.4}
$$

$$
w(t, x) = \frac{1}{2}f(x - ct) - \frac{1}{2c}G(x - ct),
\tag{2.5}
$$

such that

$$
u(t, x) = v(t, x) + w(t, x).
\tag{2.6}
$$

Each one represents a given profile moving, undisturbed, in one specific direction, v to the left and w to the right, with speed c. For instance:

$$
\begin{aligned}
v(t + \tau, x) &= \frac{1}{2}f\big((x + c(t + \tau)\big) + \frac{1}{2c}G\big((x + c(t + \tau)\big) \\
&= \frac{1}{2}f\big((x + c\tau) + ct\big) + \frac{1}{2c}G\big((x + c\tau) + ct\big) \\
&= v(t, x + c\tau),
\end{aligned}
\tag{2.7}
$$

which indicates that at a given time the profile is the same but shifted in position. If we refer this to the initial profile, we have:

$$v(t, x) = v(0, x + ct), \tag{2.8}$$

$$w(t, x) = w(0, x - ct). \tag{2.9}$$

Alternatively, we could have use Fourier techniques to split the initial data of (2.1) into the components traveling to the left and to the right. Let be $\hat{f}(\kappa)$ and $\hat{g}(\kappa)$ the Fourier transform over the whole space of, respectively, f and g. We define:

$$
\begin{aligned}
v_0(x) &= \frac{1}{\sqrt{2\pi}} \int_0^\infty \hat{f}(-\kappa) e^{-i\kappa x} d\kappa \,, \\
v_0'(x) &= \frac{1}{\sqrt{2\pi}} \int_0^\infty \hat{g}(-\kappa) e^{-i\kappa x} d\kappa \,,
\end{aligned}
\tag{2.10}
$$

and

$$
\begin{aligned}
w_0(x) &= \frac{1}{\sqrt{2\pi}} \int_0^\infty \hat{f}(\kappa) e^{i\kappa x} d\kappa \,, \\
w_0'(x) &= \frac{1}{\sqrt{2\pi}} \int_0^\infty \hat{g}(\kappa) e^{i\kappa x} d\kappa \,.
\end{aligned}
\tag{2.11}
$$

Let us consider a special case for (2.1) where both functions f and G (and, accordingly, g) have compact support, and that there exists a value $L > 0$ such that

$$\forall x, \quad |x| > L \to \begin{cases} f(x) = 0 \,, \\ G(x) = 0 \,, \end{cases} \tag{2.12}$$

which implies that

$$u(t, -L) = v(t, -L) \,, \quad u(t, L) = w(t, L) \quad \forall t \geq 0 \,. \tag{2.13}$$

This means that the region $(-\infty, -L)$ will only "see" a perturbation given by v, while the region (L, ∞) will only "see" a perturbation given by w, and that only after a certain time. Besides, the central region $(-L, L)$ will become undisturbed (u and u_t being zero for all its points) after some time, since both profiles will exit by its left side or by its right side.

For this central region we can substitute (2.1) by an equivalent problem:

$$
\begin{aligned}
\varphi_{tt} - c^2 \varphi_{xx} &= 0 \,, \quad t \geq 0, \ x \in [-L, L] \,, \\
\varphi(0, x) &= f(x) \,, \\
\varphi_t(0, x) &= g(x) \,, \\
\varphi(t, -L) &= v(0, ct - L) \,, \\
\varphi(t, L) &= w(0, L - ct) \,,
\end{aligned}
\tag{2.14}
$$

since we have

$$u(t, x) = \varphi(t, x) \,, \quad \forall t \geq 0, \ \forall x \in [-L, L] \,. \tag{2.15}$$

We may say that the boundary conditions on φ, both at L and at $-L$, are "transparent". Any other kind of boundary conditions would induce a solution φ different from u at some location inside $[-L, L]$ after some given time.

Discrete level. In practice, we cannot simulate (2.1) by finite differences due to the infinite range of x-values, but we can simulate a problem such as (2.14): we build a discrete time-space mesh given by values $t_n = n\Delta t$, $x_l = l\Delta x$, with $n \in \mathbb{N}$ and $l \in \mathbb{Z}$, and compute the values $\varphi(t_n, x_l)$, that we denote by φ_l^n.

The standard discretized equation is given by the centered, second order expression or scheme:

$$\frac{\varphi_l^{n+1} - 2\varphi_l^n + \varphi_l^{n-1}}{\Delta t^2} - c^2 \frac{\varphi_{l+1}^n - 2\varphi_l^n + \varphi_{l-1}^n}{\Delta x^2} = 0\,, \tag{2.16}$$

that we may express as

$$\varphi_l^{n+1} = 2\varphi_l^n - \varphi_l^{n-1} - \gamma^2 \left(\varphi_{l+1}^n - 2\varphi_l^n + \varphi_{l-1}^n\right)\,, \tag{2.17}$$

with

$$\gamma = \frac{c\Delta t}{\Delta x}\,. \tag{2.18}$$

The local truncation error for φ_l^{n+1} in (2.17) is:

$$-\frac{\gamma^2}{12}\,(1 - \gamma^2)\Delta x^4\,\varphi_{xxxx}(\tilde{t}, \tilde{x})\,, \tag{2.19}$$

for some intermediate values $\tilde{t}$, and $\tilde{x}$, that depend on n and l. This expression can be obtained, for instance, expanding in Taylor series around φ_l^n the different terms involved and using the mean value theorem. We see that in order to compute a given value φ_l^{n+1} we need some previous (in time) neighbouring values. We sketch this dependence with the diagram represented in Figure 1.
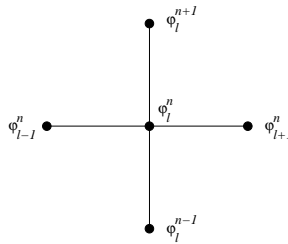
FIGURE 1. Values needed to compute φ_l^{n+1}.

Two sets of values, for $n = 0$ and $n = 1$, must be known to start the computations. They are obtained from the initial conditions. In general this can be done assuming that the solution satisfies the equation at the initial time (which is not required in theory) and performing a Taylor series expansion: for all l,

$$\begin{aligned}
\varphi_l^0 &= f(x_l)\,, \\
\varphi_l^1 &= \varphi_l^0 + \Delta t\, g(x_l) + c\,\frac{\Delta t^2}{2} f''(x_l) + c^2 \frac{\Delta t^3}{2} g''(x_l) + O(\Delta t^4)\,.
\end{aligned} \tag{2.20}$$

Truncating the $O(\Delta t^4)$ term, we obtain an approximation to the initial data of the same order in Δt as the truncation error of (2.17). On the other hand, in the case where both v and w are known, we may choose the exact values: for all l,

$$\begin{aligned}
\varphi_l^0 &= f(x_l)\,, \\
\varphi_l^1 &= u(\Delta t, x_l) = v(0, x_l + c\Delta t) + w(0, x_l - c\Delta t)\,,
\end{aligned} \tag{2.21}$$

The boundary conditions are: for all n,

$$\varphi^n_{-\ell} = v(0, ct_n - L)\,,$$
$$\varphi^n_{\ell} = w(0, L - ct_n)\,,$$
$$(2.22)$$

where $t_n = n\Delta t$ and it is necessary to choose Δx in such a way that $\ell \equiv L/\Delta x$ is a natural number.

If we consider, for instance, the case $l = -\ell + 1$ (that is, the leftmost position where the solution is to be computed) we see from Figure 1 that the boundary value $\varphi^n_{-\ell}$ is necessary to compute $\varphi^{n+1}_{-\ell+1}$. It is clear that it is not possible to compute these boundary values from the numerical scheme (2.17) and that we actually need to provide them by an independent mechanism.

For stability reasons it is convenient to choose $c\Delta t$ and Δx fulfilling certain relation, and the best choice corresponds to $\gamma = 1$ (or, equivalently, rescale the equation to have $c = 1$ and choose $\Delta t = \Delta x$), since in this case the numerical solution is exact, in the sense that φ^n_l is computed with no local truncation error (provided the initial conditions are exact), and the only possible errors arise from the numerical round-off in the computations.

3. A DIFFERENT WAY TO BUILD TRANSPARENT CONDITIONS

3.1. **Continuous level.** From the previous analysis, we see that building exact transparent boundary conditions amounts to determine the values of v and w. We can also assume (we have seen it in the discrete case but it is clear that it should also be the same in the continuous case) that the boundary conditions cannot be deduced from the evolution equation, short to solving it.

But we may try a different approach. Instead of building v and w from the initial data, we try to identify them as the solution to some specific equations. It is easy to check that v and w satisfy the equations:

$$v_t - cv_x = 0\,, \tag{3.1}$$
$$w_t + cw_x = 0\,, \tag{3.2}$$

and thus problem (2.1) can be stated equivalently as

$$u(t, x) = v(t, x) + w(t, x), \quad t \geq 0,\ x \in (-\infty, +\infty)\,,$$

$$\begin{cases} v_t - cv_x = 0\,, \\ v(0, x) = \frac{1}{2}f(x) + \frac{1}{2c}G(x)\,, \end{cases}$$

$$\begin{cases} w_t + cw_x = 0\,, \\ w(0, x) = \frac{1}{2}f(x) - \frac{1}{2c}G(x)\,. \end{cases} \tag{3.3}$$

Since both (3.1) and (3.2) are first order partial differential equations, only an initial condition is necessary, and in order to have full equivalence with (2.1) we have to impose that both v and w are sufficiently regular and satisfy their corresponding equation, either (3.1) or (3.2), at the initial time.

The interesting thing about (3.3) is that, if we build the corresponding problem for initial data with compact support, in the same way as we did for (2.1) with (2.14) we have:

$$\varphi(t, x) = \phi(t, x) + \psi(t, x), \quad t \geq 0,\ x \in [-L, L]\,,$$

$$\begin{cases} \phi_t - c\phi_x = 0 \,, \\ \phi(0,x) = \frac{1}{2}f(x) + \frac{1}{2c}G(x) \,, \\ \phi(t,-L) = \phi(0,ct-L) \,, \\ \phi(t,L) = 0 \,, \end{cases}$$

$$\begin{cases} \psi_t + c\psi_x = 0 \,, \\ \psi(0,x) = \frac{1}{2}f(x) - \frac{1}{2c}G(x) \,, \\ \psi(t,L) = \psi(0,L-ct) \,, \\ \psi(t,-L) = 0 \,, \end{cases} \tag{3.4}$$

with

$$\phi(t,x) = v(t,x) \,, \quad \psi(t,x) = w(t,x) \quad \forall x \in [-L,L] \,. \tag{3.5}$$

But, although we have two boundary conditions, in fact only one is necessary and (3.4) is equivalent to

$$\varphi(t,x) = \phi(t,x) + \psi(t,x), \quad t \geq 0, \ x \in [-L,L] \,,$$

$$\begin{cases} \phi_t - c\phi_x = 0 \,, \\ \phi(0,x) = \frac{1}{2}f(x) + \frac{1}{2c}G(x) \,, \\ \phi(t,L) = 0 \,, \end{cases} \tag{3.6}$$

$$\begin{cases} \psi_t + c\psi_x = 0 \,, \\ \psi(0,x) = \frac{1}{2}f(x) - \frac{1}{2c}G(x) \,, \\ \psi(t,-L) = 0 \,, \end{cases}$$

where both values $\phi(t,-L)$ and $\psi(t,L)$ are provided for all times by the solutions. Thus, we see that this formulation enables us to build the appropriate boundary conditions to our original problem (2.1). Also, if the values of both v and w (or, equivalently, ϕ and ψ) are known at the initial time, all references to both f or G can be suppressed in this new problem.

3.2. **Discrete level.** At discrete level the new first order equations (3.1) and (3.2) may be represented in different ways, either explicitly or implicitly, and some authors have considered different approaches [1, 2]. If we want to have a scheme that gives a similar accuracy as (2.17), we may choose a representation of the time derivative given by the second order centered difference:

$$\frac{\phi_l^{n+1} - \phi_l^{n-1}}{2\Delta t} \,. \tag{3.7}$$

In the case of the spatial derivative, if we also use the centered second order representation given by

$$\frac{\phi_{l+1}^n - \phi_{l-1}^n}{2\Delta x} \,, \tag{3.8}$$

we end with the "leap-frog" numerical scheme, which is known to be unstable, a property that rends it useless for our needs.

We start looking for a stable scheme. Let us consider the, so called, downwind method:

$$\frac{\phi_l^{n+1} - \phi_l^n}{\Delta t} - c\frac{\phi_{l+1}^n - \phi_l^n}{\Delta x} = 0 \tag{3.9}$$

$$\iff \phi_l^{n+1} = (1-\gamma)\phi_l^n + \gamma\phi_{l+1}^n \,. \tag{3.10}$$

It is stable provided $0 < \gamma \leq 1$. The inconvenient is that it is only first-order accurate, instead of second-order as (2.17). But we see that only values at l and to its right are needed. We represent the corresponding grid in Figure 2.
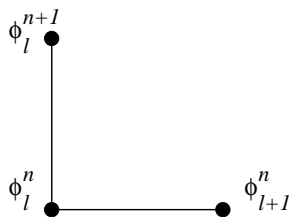
FIGURE 2. Values needed to compute ϕ_l^{n+1}.

The standard second-order stable (for $\gamma \leq 1$) numerical scheme is the Lax-Wendroff method, given by

$$\phi_l^{n+1} = \phi_l^n + \frac{\gamma}{2} \left(\phi_{l+1}^n - \phi_{l-1}^n \right) + \frac{\gamma^2}{2} \left(\phi_{l+1}^n - 2\phi_l^n + \phi_{l-1}^n \right), \tag{3.11}$$

but it has the inconvenience of using values on the left side of l. In fact, most of the good properties of this scheme (for instance, it is conservative) comes from the fact that it has a symmetric disposition of the points it uses.

We may try to build a second-order scheme that only uses points to the right. We have, for instance

$$\phi_l^{n+1} = \frac{2 - 3\gamma + \gamma^2}{2} \phi_l^n + \gamma(2 - \gamma)\phi_{l+1}^n + \frac{\gamma}{2}(1 - \gamma)\phi_{l+2}^n, \tag{3.12}$$

that has a truncation error

$$-\gamma \frac{2 - 3\gamma + \gamma^2}{6} \Delta x^3 \, \phi_{xxx}(\tilde{t}, \tilde{x}). \tag{3.13}$$

Although this looks fine, we have to understand that (2.17) being of second-order implies that the truncation error in φ_l^{n+1} is $\mathcal{O}(\Delta x^4)$, while it is only $\mathcal{O}(\Delta x^3)$ for ϕ_l^{n+1}. This is due to the fact of the continuous equation being of first order, and it means that we need not a second-order scheme but a third-order one to obtain the same kind of precision. For instance:

$$\begin{aligned} \phi_l^{n+1} &= \frac{6 - 11\gamma + 6\gamma^2 - \gamma^3}{6} \phi_l^n + \frac{6\gamma - 5\gamma^2 + \gamma^3}{2} \phi_{l+1}^n \\ &+ \frac{4\gamma^2 - 3\gamma - \gamma^3}{2} \phi_{l+2}^n + \frac{2\gamma - 3\gamma^2 + \gamma^3}{6} \phi_{l+3}^n, \end{aligned} \tag{3.14}$$

with truncation error

$$-\frac{\gamma}{24}(144 - 264\gamma + 144\gamma^2 - \gamma^3) \Delta x^4 \, \phi_{xxxx}(\tilde{t}, \tilde{x}). \tag{3.15}$$

This scheme is stable provided

$$0 < \gamma, \quad \frac{6 - 11\gamma + 6\gamma^2 - \gamma^3}{6} \leq 1, \tag{3.16}$$

which is achieved if $0 < \gamma \leq 1$ (although there are other possibilities). We represent the new grid in Figure 3.
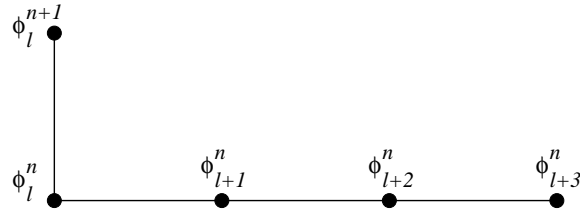
FIGURE 3. Values needed to compute ϕ_l^{n+1} with the third-order scheme (left side).

With such a numerical scheme, we may compute terms with no reference to any left hand-side boundary condition. We may combine it with the usual (and much simpler) method (2.17): we compute the values at time $n+1$ with (2.17) and then, using (3.14) with $l = \ell$, the value on the left boundary at time step $n+1$.

In this way we have transparent boundary conditions at discrete level. A similar approach can be used on the right boundary. Changing the sign of c (that is, changing the sign of γ), ϕ by ψ and inverting the relative positions with respect to l (which induces some changes in the underlying Taylor expansions), we end with:

$$\psi_l^{n+1} = \frac{6 - 11\gamma + 6\gamma^2 - \gamma^3}{6}\, \psi_l^n + \frac{6\gamma - 5\gamma^2 + \gamma^3}{2}\, \psi_{l-1}^n$$
$$+ \frac{4\gamma^2 - 3\gamma - \gamma^3}{2}\, \psi_{l-2}^n + \frac{2\gamma - 3\gamma^2 + \gamma^3}{6}\, \psi_{l-3}^n . \tag{3.17}$$

The corresponding grid is represented in Figure 4.
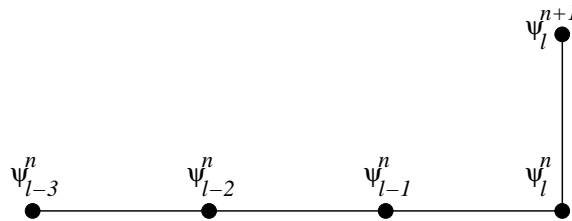
FIGURE 4. Values needed to compute ψ_l^{n+1} with the third-order scheme (right side).

In both cases, we have to assume that the only signal that is near each one of these boundaries travels in the appropriate direction. We can ensure this choosing L (and, thus, ℓ) sufficiently far away from the initial support. If we rescale the equations in order to have $c = 1$, the support is enlarged by one step in both space directions for every step in time. Thus, we only use the auxiliary schemes when $\varphi_{-\ell+1}^n$ or $\varphi_{\ell-1}^n$ are no longer zero.

By the way: if $\gamma = 1$ (3.14) and (3.17) become, respectively

$$\phi_l^{n+1} = \phi_{l+1}^n , \, \psi_l^{n+1} = \psi_{l-1}^n , \tag{3.18}$$

and the solution is, again, exact up to round-off errors, as was the case of the numerical method for the second order equation (see Section 2).

3.3. **Numerical simulations.** The idea now is to simulate the solution to (2.1) computing (2.17) and starting, for instance, with the exact initial data, and using both (3.14) and (3.17) to compute the boundary values. For this, we choose a region $[-L, L]$ wide enough, such that when the perturbation reaches any of its two ends, it is only the appropriate traveling wave that is seen there and, thus: $\varphi^n_{-\ell} = \phi^n_{-\ell}$, $\varphi^n_{\ell} = \psi^n_{\ell}$.

In the practical implementation, we may keep the values at both boundaries to zero until the wave has arrived and compute from that moment the corresponding values. Besides, only two data (those on the boundary) have to be computed, one with (3.14) and one with (3.17), and, thus, the additional computational effort is minimal: it is not necessary to keep extra variables nor to simulate new equations in the whole spatial region.
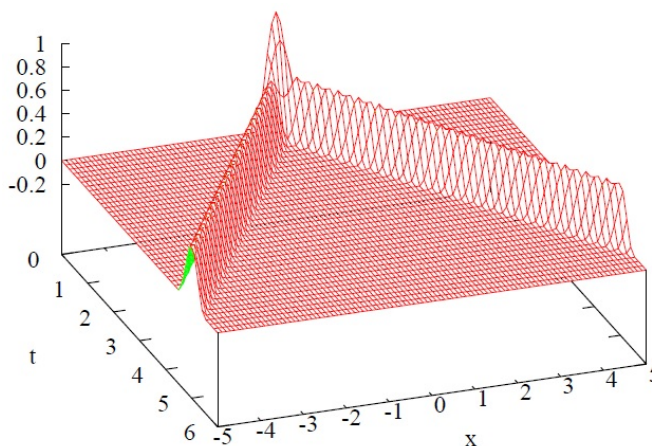
FIGURE 5. Simulation of transparent boundary conditions for the wave equation, $c = 1$, $\gamma = 1$

In Figure 5 we represent the simulation with $c = 1$, $\gamma = 1$ of the evolution of an initial profile given by

$$u(t, x) = \begin{cases} \frac{1 - \cos(\pi(x - ct)/2)}{4} + \frac{1 - \cos(\pi(x + ct)/2)}{4}, & \text{if } 0 < |x - t| \leq 1, \\ 0 & \text{otherwise.} \end{cases} \quad (3.19)$$

It corresponds to two similar traveling waves, one moving to the left, one to the right. We see that there is no disturbance due to the boundary conditions and the signal vanishes as it passes through the border. To check the influence of the numerical errors, in Figure 6 we represent the evolution of the same profile but simulated with $c = 1/2$, $\gamma = 0.5$.

We see no difference in behaviour, although the number of iterations has doubled (since the new step-time has been halved), and the signal leaves the central zone with no effect caused by the border.

4. SPINOR-LIKE FORMALISM

One-way wave equations are partial differential equation that permits wave propagation only in certain directions. Engquist and Majda [4] derived a theory to
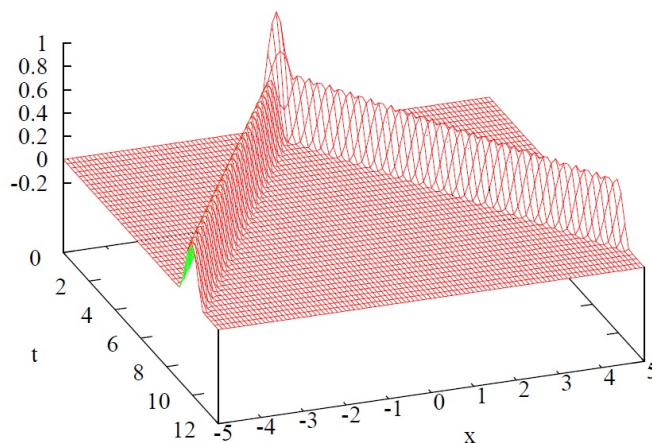
FIGURE 6. Simulation of transparent boundary conditions for the wave equation, $c = 1/2$, $\gamma = 0.5$

construct absorbing boundary conditions by factoring the wave equation

$$u_{tt} - c^2 u_{xx} = 0 \tag{4.1}$$

into two different *one-way* differential equations (for a detailed factorization see [3, 1, 4, 5])

$$u_t \pm c\sqrt{u_{xx}} = 0, \tag{4.2}$$

where $\sqrt{u_{xx}}$ represents a pseudo-differential operator that is not local in the space variable. Due to this fact, this operator, in one and higher dimensions, must be approximated using a wide variety of equations involving higher order derivatives [5, 1, 6] and in some cases this give rise to an ill-posed boundary problem [7, 8]. More recently Ionescu and Igel [2] proposed a different factorization of the wave equation valid only for spherical coordinates.

In 1928, in a completely different context, in order to avoid this complex formulation, and in his search for a covariant expression of the Schrödinger equation [9], Dirac proposed a matrix and vector (or *spinor*) formalism. In two dimensions it amounts to look for matrices 2×2, A and D, such that:

$$\frac{\partial^2}{\partial x^2} - \frac{1}{c^2}\frac{\partial^2}{\partial t^2} = \left(A\partial_x + \frac{i}{c}D\partial_t\right)^2$$
$$= A^2\partial_{xx} + \frac{i}{c}(AD + DA)\partial_{tx} - \frac{1}{c}D^2\partial_{tt}. \tag{4.3}$$

To recover the wave equation from the previous expression, A and D must satisfy the following algebra:

$$A^2 = I,$$
$$D^2 = I, \tag{4.4}$$
$$AD + DA = O.$$

Solutions are obtained taking A and D among the three Pauli matrices:

$$\sigma_1 = \begin{pmatrix} 0 & 1 \\ 1 & 0 \end{pmatrix}, \quad \sigma_2 = \begin{pmatrix} 0 & -i \\ i & 0 \end{pmatrix}, \quad \sigma_3 = \begin{pmatrix} 1 & 0 \\ 0 & -1 \end{pmatrix}, \tag{4.5}$$

for instance:

$$A = \begin{pmatrix} 0 & -i \\ i & 0 \end{pmatrix}, \quad D = \begin{pmatrix} 1 & 0 \\ 0 & -1 \end{pmatrix}. \tag{4.6}$$

This kind of ideas has been used in different contexts, resulting in interesting formulations for differential models (see, for instance, [10, 11, 12]).

The method is very general and in principle it could be extended to decompose differential operators of a least second order and it also could be applied to the hyperbolic and parabolic problems in the spirit of computing general roots of an operator indicated in [10]. A priori the main problem could be an algebraic one associated to the implementation of a certain algebra as it is indicated in [10] with the Silvester algebra. In this process a new differential equation is generated where the unknown function now is multicomponent.

The decomposition of the differential operators can be used for nonlinear problems but in that case the boundary includes some border effects that cannot be addressed directly by this linear approach.

We shall apply similar ideas in what follows to transform the wave equation into a set of one-way differential equations. Choosing the representation for the matrices, it is possible to decompose the problem into waves traveling in opposite directions as is done with the other implementations.

We start by splitting the initial data of (2.1) into the components traveling to the left and to the right, as given in the previous section, and define

$$U_0(x) = \begin{pmatrix} v_0(x) \\ w_0(x) \end{pmatrix}, \quad U_0'(x) = \begin{pmatrix} v_0'(x) \\ w_0'(x) \end{pmatrix}. \tag{4.7}$$

We also define U, a two-component vector,

$$U(t,x) = \begin{pmatrix} v(t,x) \\ w(t,x) \end{pmatrix}, \tag{4.8}$$

with v and w two real functions. We shall show that they correspond to the left and right traveling components of the solution of (2.1), when the following problem is considered

$$U_t \pm cMU_x = \mathcal{O}, \quad t \geq 0, \ x \in (-\infty, +\infty),$$
$$U(0,x) = U_0(x), \tag{4.9}$$
$$U_t(0,x) = U_0'(x),$$

where $\mathcal{O}$ stands for the null vector and M is an involutory matrix, i.e., such that $M^2 = I$. We have that

$$u(t,x) = v(t,x) + w(t,x), \quad \forall t \geq 0, \ \forall x \in (-\infty, \infty), \tag{4.10}$$

with $u(t,x)$ the solution of (2.1). Indeed, assuming U to be regular enough, on the one hand we have

$$U_t \pm cMU_x = \mathcal{O} \rightarrow U_{tt} \pm cMU_{xt} = \mathcal{O}$$
$$\iff U_{tt} \pm cMU_{tx} = \mathcal{O}$$
$$\iff U_{tt} - c^2 M^2 U_{xx} = \mathcal{O} \tag{4.11}$$
$$\iff \left\{ \begin{array}{l} v_{tt} - c^2 v_{xx} = 0, \\ w_{tt} - c^2 w_{xx} = 0, \end{array} \right\}$$

and on the other hand,

$$\left\{ \begin{array}{l} v_0(x) + w_0(x) = f(x)\,, \\ v_0'(x) + w_0'(x) = g(x)\,, \end{array} \right\} \iff \left\{ \begin{array}{l} v(0, x) + w(0, x) = u(0, x)\,, \\ v_t(0, x) + w_t(0, x) = u_t(0, x)\,. \end{array} \right\} \tag{4.12}$$

We see that equation (4.2) can be expressed using the Dirac-like equation of the initial value and boundary problem (4.9), considering a two-dimensional real quantity $U(t, x)$ as the variable. Due to its transformation properties, and following with the Dirac analogy, we may call it a *spinor*. We may now transform our original problem (2.1) into (4.9). Since the sign that appears in the equation is irrelevant, we have chosen a positive sign, and our "Dirac equation" for this case is, finally,

$$U_t + cMU_x = \mathcal{O}. \tag{4.13}$$

Although our procedure looks different from (4.3) and (4.4), it can be shown to be similar, just considering an appropriate M. For instance, if we chose A and D as in (4.6), we have $M = -iAD^{-1}$, a real involutory matrix.

Involutory matrices of dimensions 2×2 are of two kinds: $M = \pm I$ or

$$M = \pm \begin{pmatrix} a & \beta \\ \delta & -a \end{pmatrix} \tag{4.14}$$

with $\beta\delta = 1 - a^2$. Choosing a specific matrix M is equivalent to fixing the Dirac gauge. We shall consider in what follows only symmetric matrices, for sake of simplicity. This supposes that, besides the somewhat trivial choices $\pm I$, matrix M is of the form

$$M = \begin{pmatrix} \sin\alpha & \cos\alpha \\ \cos\alpha & -\sin\alpha \end{pmatrix} \tag{4.15}$$

with α is some angle to be fixed if necessary. An involutory, symmetric, matrix is orthogonal and we see that our choice of M corresponds to the matrix of a reflection.

Incident wave at $x = -L$. An incident wave at $x = -L$ with negative wave number is represented in this case by

$$U_I = \begin{pmatrix} a \\ b \end{pmatrix} e^{i(\omega t + kx)}, \quad k > 0. \tag{4.16}$$

Such a wave induces, due to reflection at the boundary $x = -L$, a reflected plane wave traveling backwards of the form

$$U_R = T \begin{pmatrix} a \\ b \end{pmatrix} e^{i(\omega t + kx)} + R \begin{pmatrix} a \\ b \end{pmatrix} e^{i(\omega t - kx)}, \tag{4.17}$$

where T and R are, respectively, the transmission and the reflection coefficients.

It can be checked that at the boundary $x = -L$ we have

$$\partial_x U_R = ik(Te^{-ikL} - Re^{ikL}) \begin{pmatrix} a \\ b \end{pmatrix} e^{i\omega t}, \tag{4.18}$$

$$\partial_t U_R = i\omega(Te^{-ikL} + Re^{ikL}) \begin{pmatrix} a \\ b \end{pmatrix} e^{i\omega t}.$$

Introducing (4.17) and (4.18) into (4.13) and setting $x = -L$, we obtain the linear algebraic system

$$[\omega(Te^{-ikL} + Re^{ikL})I - ck(Te^{-ikL} - Re^{ikL})M] \begin{pmatrix} a \\ b \end{pmatrix} = 0\,. \tag{4.19}$$

This equation results from considering that the superposition of transmitted and reflected waves coincides at the boundary and that the Dirac equation (4.13) holds.

Different representations of matrix M result in different equations. Trivial cases are $M = I$, that gives the condition $R = 0$, and $M = -I$, that gives the condition $T = 0$. These two cases are trivial since they correspond to the Dirac form of the scalar square root of the wave equation and represent waves traveling in one single direction. These cases are trivial but useless since what we want is to decompose the wave packet into its left and right-traveling parts.

A nontrivial case arises when other possible forms of matrix M are used, and the necessary condition for system (4.19) to have a nontrivial solution corresponds to annihilate the determinant of its matrix,

$$
\begin{aligned}
&\left| \omega(Te^{-ikL} + Re^{ikL})I - ck(Te^{-ikL} - Re^{ikL})M \right| = 0 \\
&\iff (\omega^2 - c^2k^2)(T^2e^{-2ikL} + R^2e^{2ikL}) + 2RT(w^2 + c^2k^2) = 0 \,.
\end{aligned}
\tag{4.20}
$$

Given the dispersion relation for the plane-waves,

$$
\omega^2 = c^2k^2;
\tag{4.21}
$$

this equation has two solutions, $R = 0$, $T \in \mathbb{R}$, and $T = 0$, $R \in \mathbb{R}$.

In the two trivial cases $M = \pm I$, since the system has a diagonal matrix, all the spinors are solutions of (4.19).

In other representations of matrix M, special spinors solutions can be found for null values of T and R. These spinors are the "special directions" for the operators "transmission" and "reflection". If we look for spinors associated to every value of the reflection coefficient obtained with the others realizations of matrix M, we have for $R = 0$,

$$
\Psi_T = \begin{pmatrix} a \\ b \end{pmatrix} = \begin{pmatrix} 1 \\ \frac{1-\sin\alpha}{\cos\alpha} \end{pmatrix} a \,,
\tag{4.22}
$$

and for $R = 1$,

$$
\Psi_R = \begin{pmatrix} a \\ b \end{pmatrix} = \begin{pmatrix} 1 \\ \frac{-1-\sin\alpha}{\cos\alpha} \end{pmatrix} a \,.
\tag{4.23}
$$

Then matrix M can be diagonalized in the basis of vectors

$$
\mathcal{B} = \{U_1, U_2\}, \quad U_1 = \begin{pmatrix} -\cos\alpha \\ \sin\alpha - 1 \end{pmatrix}, \quad U_2 = \begin{pmatrix} -\cos\alpha \\ \sin\alpha + 1 \end{pmatrix},
\tag{4.24}
$$

with canonical form

$$
D = \begin{pmatrix} 1 & 0 \\ 0 & -1 \end{pmatrix}.
\tag{4.25}
$$

It is possible to see that at $x = -L$, the component along vector U_2 is not transmitted to the left, while the component along U_1 passes without distortion. We may, in this way, obtain transparent boundary conditions at $x = -L$. Let us consider our solution to (4.9). We decompose the vector in the basis $\mathcal{B}$:

$$
U = a_1 U_1 + a_2 U_2 \iff \begin{pmatrix} a_1 \\ a_2 \end{pmatrix} = NU, \quad N = \frac{1}{2\cos\alpha} \begin{pmatrix} -\sin\alpha - 1 & -\cos\alpha \\ \sin\alpha - 1 & \cos\alpha \end{pmatrix},
$$

and we can establish the dynamics for each component:

$$(a_1)_{tt} - c^2(a_1)_{xx} = 0, \quad t \geq 0, \ x \in (-\infty, +\infty),$$
$$a_1(0, x) = -\frac{\sin\alpha + 1}{2\cos\alpha}v_0(x) - \frac{1}{2}w_0(x),$$
$$(a_1)_t(0, x) = -\frac{\sin\alpha + 1}{2\cos\alpha}v_0'(x) - \frac{1}{2}w_0'(x),$$

(4.26)

and

$$(a_2)_{tt} - c^2(a_2)_{xx} = 0, \quad t \geq 0, \ x \in (-\infty, +\infty),$$
$$a_2(0, x) = \frac{\sin\alpha - 1}{2\cos\alpha}v_0(x) + \frac{1}{2}w_0(x),$$
$$(a_2)_t(0, x) = \frac{\sin\alpha - 1}{2\cos\alpha}v_0'(x) + \frac{1}{2}w_0'(x),$$

(4.27)

or, in spinor form, if we define $V = NU$:

$$V_t + cDV_x = 0, \quad t \geq 0, \ x \in (-\infty, +\infty),$$
$$V(0, x) = NU_0(x),$$
$$V_t(0, x) = NU_0'(x),$$

(4.28)

where

$$N^{-1} = \begin{pmatrix} -\cos\alpha & -\cos\alpha \\ \sin\alpha - 1 & \sin\alpha + 1 \end{pmatrix},$$

(4.29)

and $D = NMN^{-1}$ is the canonical form (4.25).

Finally we have

$$u(t, x) = \begin{pmatrix} 1 & 1 \end{pmatrix}\begin{pmatrix} v \\ w \end{pmatrix} = \begin{pmatrix} 1 & 1 \end{pmatrix}N^{-1}\begin{pmatrix} a_1 \\ a_2 \end{pmatrix}$$
$$= -(1 - \sin\alpha + \cos\alpha)a_1(t, x) + (1 + \sin\alpha - \cos\alpha)a_2(t, x).$$

(4.30)

The special spinor problem (4.28) represents a pair of independent waves, $a_1(x, t) = a_1(x + ct)$ traveling to the left, and another $a_2(x, t) = a_2(x - ct)$ traveling to the right.

When the signal reaches the left boundary, the a_1 component vanishes and if we want the whole signal also to vanish to the left of $-L$, we may choose $\alpha = 2k\pi$ or $\alpha = \frac{3\pi}{2} + 2k\pi$, $k = 1, 2, 3, \ldots$

The first choice ($\alpha = 2k\pi$, $k = 1, 2, 3, \ldots$) corresponds to

$$M = \begin{pmatrix} 0 & 1 \\ 1 & 0 \end{pmatrix},$$

(4.31)

which is equivalent to the coupled formulation of the wave equation

$$v_t + cw_x = 0$$
$$w_t + cv_x = 0.$$

(4.32)

In this case the basis of spinors is:

$$\Psi_T = \begin{pmatrix} 1 \\ 1 \end{pmatrix}, \quad \Psi_R = \begin{pmatrix} 1 \\ -1 \end{pmatrix}.$$

(4.33)

For the second choice ($\alpha = \frac{3\pi}{2} + 2k\pi$, $k = 1, 2, 3, \ldots$), we particularize the calculus for the case in which the waves are decomposed. By reformulating from

the beginning we obtain the spinors:

$$\Psi_T = \begin{pmatrix} 1 \\ 0 \end{pmatrix} a \,, \tag{4.34}$$

and for $R = 1$,

$$\Psi_R = \begin{pmatrix} 0 \\ 1 \end{pmatrix} a \,. \tag{4.35}$$

Expressing now the spinor formalism for these new values, we obtain as matrix

$$M = \begin{pmatrix} -1 & 0 \\ 0 & 1 \end{pmatrix}. \tag{4.36}$$

This uncouples the equations into two one-dimensional wave equations, that are just the ones treated in Section 3.1. We thus see that the spinor formalism is a natural way to decompose the original problem into its components and to obtain the first-order differential equations we have used before. Numerical simulations can then be performed using the Lax-Wendroff scheme with the third-order scheme at the corresponding boundary end. In Figures 7 and 8, we have represented the numerical solution for the left and right-traveling components (same initial values as before): there are no reflections at the boundaries when the waves reach them.
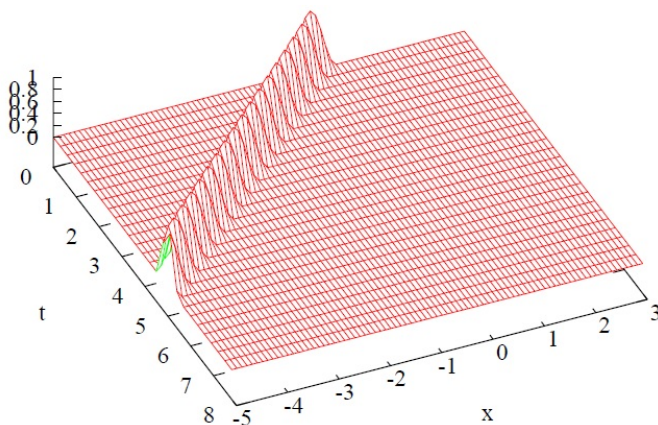
FIGURE 7. Simulation of transparent boundary conditions for the Dirac Equation, $c = 1$, $\gamma = 1$, left-traveling wave.

4.1. **Incident wave at $x = L$.** We treat now the case of the incident wave at the opposite boundary. All the computations are similar to what is done Section 4, but they involve an incident wave at $x = L$ with positive wave number, represented by

$$U_I = \begin{pmatrix} a \\ b \end{pmatrix} e^{i(\omega t - kx)}, \quad k > 0. \tag{4.37}$$

The reflected wave at the other boundary is now:

$$U_R = T \begin{pmatrix} a \\ b \end{pmatrix} e^{i(\omega t - kx)} + R \begin{pmatrix} a \\ b \end{pmatrix} e^{i(\omega t + kx)}, \tag{4.38}$$
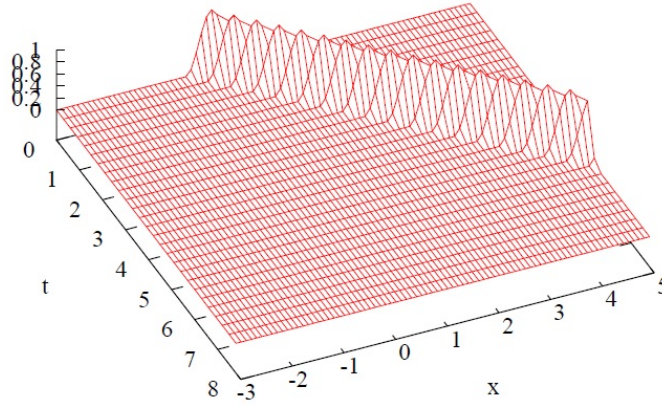
FIGURE 8. Simulation of transparent boundary conditions for the
Dirac Equation, $c = 1$, $\gamma = 1$, right-traveling wave.

and at the boundary $x = L$ we have

$$\partial_x U_R = ik(-Te^{-ikL} + Re^{ikL})\begin{pmatrix} a \\ b \end{pmatrix} e^{i\omega t},$$

$$\partial_t U_R = i\omega(Te^{-ikL} + Re^{ikL})\begin{pmatrix} a \\ b \end{pmatrix} e^{i\omega t}. \tag{4.39}$$

We follow what was done in 4, and obtain at $x = L$ the linear algebraic system

$$[\omega(Te^{-ikL} + Re^{ikL})I - ck(-Te^{-ikL} + Re^{ikL})M]\begin{pmatrix} a \\ b \end{pmatrix} = 0. \tag{4.40}$$

Here again, different choices for the matrix M will result in different equations.
The trivial case $M = I$ gives the condition $T = 0$ while the second trivial case,
with $M = -I$, gives the condition $R = 0$.

With some other form for matrix M we obtain non trivial cases. We annihilate
the determinant of system (4.40) to obtain a necessary condition for a nontrivial
solution:

$$\left|\omega(Te^{-ikL} + Re^{ikL})I - ck(-Te^{-ikL} + Re^{ikL})M\right| = 0$$

$$\Longleftrightarrow (\omega^2 - c^2k^2)(T^2 e^{-2ikL} + R^2 e^{2ikL}) + 2RT(w^2 + c^2k^2) = 0. \tag{4.41}$$

The two solutions are, as in the other boundary, $R = 0$ and $T = 0$.

In the two trivial cases mentioned above, $M = \pm I$, all the spinors are solutions
of (4.40). In the nontrivial case, we have for $R = 0$:

$$\Psi_T = \begin{pmatrix} a \\ b \end{pmatrix} = \begin{pmatrix} 1 \\ \frac{-1-\sin\alpha}{\cos\alpha} \end{pmatrix} a, \tag{4.42}$$

and for $R = 1$:

$$\Psi_R = \begin{pmatrix} a \\ b \end{pmatrix} = \begin{pmatrix} 1 \\ \frac{1-\sin\alpha}{\cos\alpha} \end{pmatrix} a. \tag{4.43}$$

The basis of spinors in which M is diagonal is now

$$\mathcal{B} = \{U_1, U_2\}, \quad U_1 = \begin{pmatrix} -\cos\alpha \\ 1+\sin\alpha \end{pmatrix}, \quad U_2 = \begin{pmatrix} -\cos\alpha \\ \sin\alpha - 1 \end{pmatrix}, \tag{4.44}$$

and the canonical form is

$$D = \begin{pmatrix} -1 & 0 \\ 0 & 1 \end{pmatrix}. \tag{4.45}$$

At $x = L$, the component along vector U_2 is not transmitted to the right, while the component along U_1 passes without distortion, which correspond to the transparent boundary conditions at $x = L$. Decomposing the solution to (4.9) in this new basis, we have

$$U = a_1 U_1 + a_2 U_2 \iff \begin{pmatrix} a_1 \\ a_2 \end{pmatrix} = NU, \quad N = \frac{1}{2\cos\alpha} \begin{pmatrix} \sin\alpha - 1 & \cos\alpha \\ -(1+\sin\alpha) & -\cos\alpha \end{pmatrix}.$$

The dynamics for each component corresponds to

$$(a_1)_{tt} - c^2(a_1)_{xx} = 0, \quad t \geq 0, \ x \in (-\infty, +\infty),$$

$$a_1(0,x) = \frac{\sin\alpha - 1}{2\cos\alpha} v_0(x) + \frac{1}{2} w_0(x), \tag{4.46}$$

$$(a_1)_t(0,x) = \frac{\sin\alpha - 1}{2\cos\alpha} v_0'(x) + \frac{1}{2} w_0'(x),$$

and to

$$(a_2)_{tt} - c^2(a_2)_{xx} = 0, \quad t \geq 0, \ x \in (-\infty, +\infty),$$

$$a_2(0,x) = -\frac{1+\sin\alpha}{2\cos\alpha} v_0(x) - \frac{1}{2} w_0(x), \tag{4.47}$$

$$(a_2)_t(0,x) = -\frac{1+\sin\alpha}{2\cos\alpha} v_0'(x) - \frac{1}{2} w_0'(x).$$

Represented in spinor form, with $V = NU$, this gives

$$V_t + cDV_x = 0, \quad t \geq 0, \ x \in (-\infty, +\infty),$$

$$V(0,x) = NU_0(x), \tag{4.48}$$

$$V_t(0,x) = NU_0'(x),$$

where

$$N^{-1} = \begin{pmatrix} -\cos\alpha & -\cos\alpha \\ 1+\sin\alpha & \sin\alpha - 1 \end{pmatrix}, \tag{4.49}$$

and $D = NMN^{-1}$ is the canonical form (4.45).

Although this looks exactly the same as (4.28), it is necessary to point out that, here, the diagonal matrix D is the opposite to (4.25). Also, the matrix N and its inverse N^{-1} have changed. This is clearly seen in our final representation of the solution

$$u(t,x) = \begin{pmatrix} 1 & 1 \end{pmatrix} \begin{pmatrix} v \\ w \end{pmatrix} = \begin{pmatrix} 1 & 1 \end{pmatrix} N^{-1} \begin{pmatrix} a_1 \\ a_2 \end{pmatrix}$$

$$= (1 + \sin\alpha - \cos\alpha) a_1(t,x) - (1 - \sin\alpha + \cos\alpha) a_2(t,x). \tag{4.50}$$

The interpretation is now that problem (4.48), in spinor form, represents a pair of independent waves, $a_1(x,t) = a_1(x + ct)$ traveling to the right, and another $a_2 = a_2(x - ct)$ traveling to the left. Such that when the signal reaches the right boundary, the a_1 component is lost. If we want the whole signal to vanish to the right of L, we may choose $\alpha = \frac{\pi}{2} + 2n\pi$ or $\alpha = \pi + 2n\pi$, $n = 1, 2, 3, \ldots$

As before, if we choose $\alpha = \frac{\pi}{2} + 2n\pi$, $n = 1, 2, 3, \ldots$, it is necessary to reformulate the spinors:

$$\Psi_T = \begin{pmatrix} 0 \\ 1 \end{pmatrix})a, \tag{4.51}$$

and for $R = 1$,

$$\Psi_R = \begin{pmatrix} 1 \\ 0 \end{pmatrix} a. \tag{4.52}$$

With the new spinors, matrix M is now

$$M = \begin{pmatrix} 1 & 0 \\ 0 & -1 \end{pmatrix}. \tag{4.53}$$

Once again, this uncouples the equations into two one-dimensional wave equations, that are just the ones treated in Section 3.1.

The other values of $\alpha = \pi + 2n\pi$, $n = 1, 2, 3, \ldots$, give raise, again, to the coupled formulation for the wave equation

$$\begin{aligned} v_t - cw_x &= 0 \\ w_t - cv_x &= 0, \end{aligned} \tag{4.54}$$

with the same spinors Ψ_T and Ψ_R written in (4.33).

5. Wave equation in three dimensions with radial symmetry
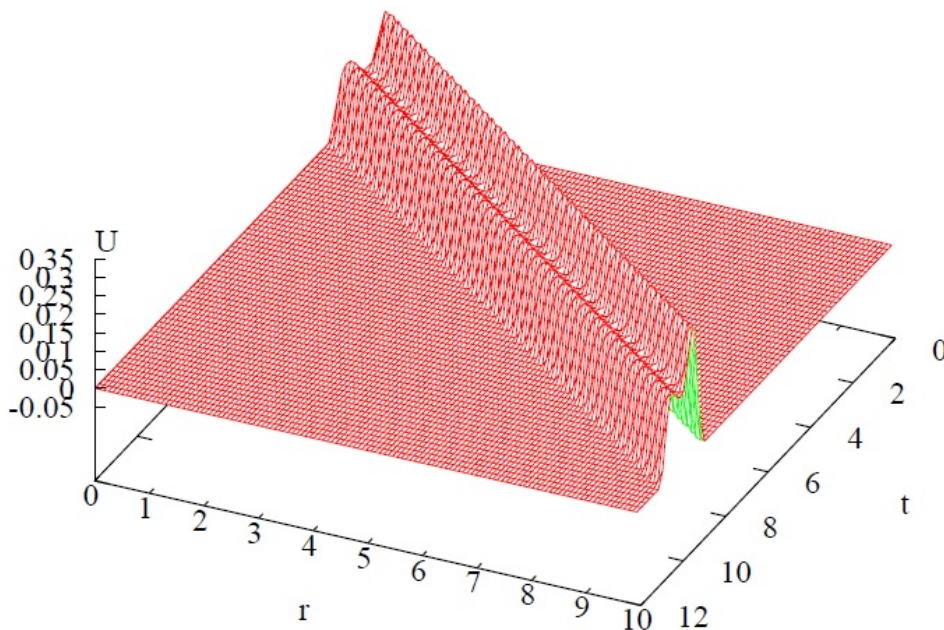
FIGURE 9. Computation of $\mathcal{U}(t, r)$ with a transparent boundary condition at $r = 10$.

Let us consider the wave equation in three dimensions with radial symmetry. We have

$$\begin{aligned} u_{tt} - c^2 \Delta u = 0 &\iff u_{tt} - c^2 \frac{1}{r^2} \frac{\partial}{\partial r} \left(r^2 u_r \right) = 0 \\ &\iff u_{tt} - c^2 \left(u_{rr} + \frac{2}{r} u_r \right) = 0. \end{aligned} \tag{5.1}$$
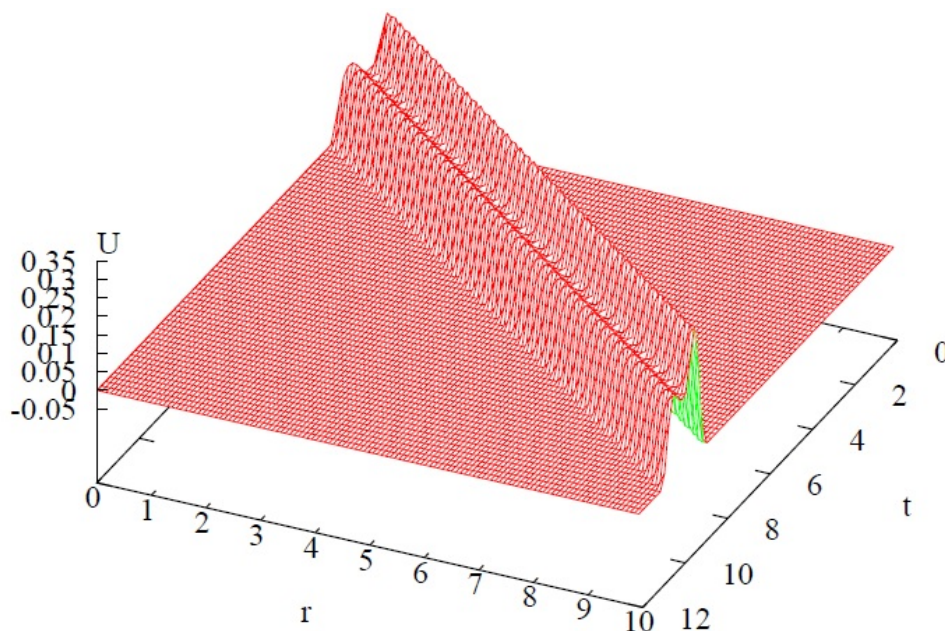
FIGURE 10. Computation of $u(t, r)$ with a transparent boundary condition at $r = 10$.

Performing the change: $\mathcal{U} = ru$, we have

$$\mathcal{U}_{tt} - c^2 \mathcal{U}_{rr} = 0, \tag{5.2}$$

and we may use the previous results in one spatial dimension to create the corresponding transparent boundary conditions. If we consider an initial value problem with radial symmetry, we can express it in terms of the new function as:

$$\left\{ \begin{array}{l} u_{tt} - c^2 \left(u_{rr} + \frac{2}{r} u_r \right) = 0, \\ t \geq 0, \ r \in [0, +\infty), \\ u(0, r) = f(r), \\ u_t(0, r) = g(r), \end{array} \right\} \iff \left\{ \begin{array}{l} \mathcal{U}_{tt} - c^2 \mathcal{U}_{rr} = 0, \\ t \geq 0, \ r \in [0, +\infty), \\ \mathcal{U}(0, r) = rf(r), \\ \mathcal{U}_t(0, r) = rg(r), \end{array} \right\} \tag{5.3}$$

In this case, if we suppose that the initial data is regular at he origin, and thus that $\forall t$, $u_r(t, 0) = 0$ due to the radial symmetry, we have a left boundary condition given by

$$\mathcal{U}(t, 0) = \lim_{r \to 0} ru(t, r) = 0, \quad \forall t. \tag{5.4}$$

On the other hand, since

$$\mathcal{U}_r(t, r) = u(t, r) + ru_r(t, r), \tag{5.5}$$

we have, also by the regularity of the functions,

$$\mathcal{U}_r(t, 0) = \lim_{r \to 0} \Big(u(t, r) + ru_r(t, r) \Big) = u(t, 0), \quad \forall t. \tag{5.6}$$

This may be used to reconstruct $u(t, r)$ from $\mathcal{U}(t, r)$ at $r = 0$, since this value cannot be obtained directly inverting the change. Some other conditions can be derived

for the derivatives of $\mathcal{U}$ at $r = 0$. For instance,

$$\mathcal{U}_t(t,0) = 0\,, \quad \mathcal{U}_{rr}(t,0) = 0\,, \quad \mathcal{U}_{tt}(t,0) = 0 \quad \forall t\,.$$

In this radial symmetry case, the waves can only travel towards the right from the origin $r = 0$, but this does not exclude the possibility of the initial data having some traveling component moving leftwards, towards the origin. Nevertheless, if the initial data is of compact support, after some time all the signal will be traveling to the right of the origin. We may thus establish a transparent boundary condition at some suitable distance.

As for the numerical simulations, we may use the previous schemes, (2.17) for the general case with a left boundary condition at the origin, and (3.17) at the right boundary.

In Figures 9 and 10 we represent, respectively, the profiles of $\mathcal{U}$ and u for the initial data,

$$u(t,r) = \begin{cases} \frac{1-\cos(\pi(r-ct)/2)}{4} - \frac{1-\cos(\pi(r+ct)/2)}{8}\,, & \text{if } 0 < |r - t| \le 1, \\ 0 & \text{otherwise.} \end{cases} \tag{5.7}$$

computed with $c = 1$ and $\gamma = 1$. This last figure shows the decay in the amplitude of the solution as the signal travels away from the origin.

It is clear that we may also apply the spinor formalism of Section 4 to equation (5.2) and achieve the same results but under the alternative formulation.

References

[1] B. Engquist, L. Halpern; *Long-time Behaviour of Absorbing Boundary Conditions*, Mathematical Methods in the Applied Sciences, 13 (1990), 189–203.

[2] D.-C. Ionescu, H. Igel; *Transparent Boundary Conditions for Wave Propagation on Unbounded Domains*, Computational Science – ICCS 2003 Lecture Notes in Computer Science, 2659 (2003), 807–816.

[3] R. Clayton, B. Engquist; *Absorbing boundary conditions for acoustic and elastic wave equations*, Bull. Seis. Sot. Am., 67 (1977), 1524–1540.

[4] B. Engquist, A. Majda; *Absorbing boundary conditions for the numerical simulation of waves*, Math. Comp., 31 (139) (1977), 629–651.

[5] A. Taflove, S. C. Hagness; *Computational Electrodynamics: The finite difference time-domain method*, Artech House, 2000.

[6] L. Trefethen, L. Halpern; *Well-Posedness of One-Way wave equations and Absorbing Boundary Conditions*, Math. Comp., 47(176) (1986), 421–435.

[7] L. Halpern; *Absorbing Boundary Conditions for the Discretization Schemes of the One-Dimensional Wave Equation*, Math. Comp., 28(158) (1982), 415–429.

[8] L. Trefethen; *Finite Difference and Spectral Methods for Ordinary and Partial Differential Equations*, Cornell University [Department of Computer Science and Center for Applied Mathematics], 1996.

[9] P. A. M. Dirac; *The Quantum Theory of the Electron*, Proceedings of the Royal Society of London, Series A1, 117(778) (1928), 610–624.

[10] L. Vázquez; *Fractional diffusion equation with internal degrees of freedom*, Jour. of Comp. Math., 21 (2003), 491-494.

[11] Pierantozzi, L. Vázquez; *An interpolation between the wave and diffusion equations through the fractional evolution equations Dirac like*, Jour. of Math. Phys., 46 (2005), 1135123.

[12] L. Vázquez; *A Fruitful Interplay: From Nonlocality to Fractional Calculus*, in V.V. Konotop, F. Abdullaev (Eds.), Nonlinear Waves, Classical and Quantum Aspects, NATO Science Series, Kluwer Academic Publishers 2004, pp. 129-133.

M. Pilar Velasco
Área de Matemáticas, Estadística e Investigación operativa, Centro Universitario de la Defensa, Academia General Militar, 50090 Zaragoza, Spain
  E-mail address: `velascom@unizar.es`

David Usero
Sección Departamental de Matemática Aplicada, Facultad de CC. Químicas, Universidad Complutense de Madrid, 28040 Madrid, Spain
  E-mail address: `umdavid@mat.ucm.es`

Salvador Jiménez
Departamento de Matemática Aplicada a las TT. II., E.T.S.I. Telecomunicación, Universidad Politécnica de Madrid, 28040 Madrid, Spain
  E-mail address: `s.jimenez@upm.es`

Luis Vázquez
Departamento de Matemática Aplicada, Facultad de Informática, Universidad Complutense de Madrid, 28040 Madrid, Spain
  E-mail address: `lvazquez@fdi.ucm.es`